Optical Fiber Bragg Grating Sensors for Torque Induced Strain Monitoring in Filament Wound Composite Shafts

M. Konstantaki[a], G. Violakis[a], T. Geernaert[b,d], N. Korakas[a], N. Tiriakidis[c], Th. Tiriakidi[c], K. Tiriakidis[c], H. Thienpont[b,d], F. Berghmans[b,d], S. Pissadakis[a]

[a] *Institute of Electronic Structure and Laser (IESL), Foundation for Research and Technology- Hellas (FORTH), N. Plastira 100, 700 13 Heraklion, Crete, Greece*

[b] *Vrije Universiteit Brussel, Pleinlaan 2, 1050, Brussels, Belgium*

[c] *BT Composites S. A., Agrokthma Florina AA 1834, 53100 Florina, Greece*

[d] *Flanders Make, Oude Diestersebaan 133, 3920 Lommel, Belgium*

Contact author e-mail: mkonst@iesl.forth.gr

Abstract: Optical fiber Bragg gratings are embedded within the composite lay-up of drive shafts during filament winding for monitoring vital operational parameters including buckling. We report strain measurement results, under torque loading, for embedded and externally attached sensors with different orientations with respect to the axis of the shaft.

OCIS codes: (060.2370) Fiber optics sensors; (060.3735) Fiber Bragg gratings; (120.4290) Nondestructive testing;

1. Introduction

Carbon fiber composites are increasingly used in several applications due to their exceptional mechanical characteristics such as lightweight, high stiffness-to-weight ratio, low thermal expansion, excellent corrosion and fatigue resistance. Hollow cylindrical composite structures manufactured by filament winding, in particular, are used extensively as torque transmission shafts, process pipes and pressure housing cylinders in automotive, marine and industrial applications. Filament winding enables the production of shafts with very small thickness (compared to their diameter) and allows for flexibility in determining the structural properties of the final product.

A supplemental advantage of composite materials is their ability to host smart sensors such as optical fiber based sensors (OFSs) within their woven structure, for monitoring vital mechanical parameters during their operation [1, 2]. OFSs can be can be embedded into or attached onto the composite structure in a minimally intrusive manner, whilst providing for high measurement sensitivity. Fiber Bragg Grating (FBG) based sensors, in particular, are easily multiplexed and have many advantages including a linear response. They have attracted considerable interest for supporting Structural Health Monitoring (SHM) applications of composite structures [3, 4].

In this report we focus on transmission torque composite shafts that can experience buckling during operation. This deformation may lead to mechanical failure of such a type of structures. To monitor the loads during torque transmission we have incorporated FBGs during actual on-site [5] filament winding of hollow cylindrical shafts in view of the future development of buckling sensors. We embedded FBGs along different orientations with respect to the axis of the shaft to determine the optimum layout for monitoring possible buckling effects under quasi-static torque. We also mounted FBGs to the shaft surface for comparison.

2. Experimental

We inscribed FBGs in Nufern GF1B optical fiber using a standard phase mask setup, with a 193 nm high spatial coherence and 10 ns pulse duration excimer laser (Braggstar, TUI laser), with a pulse energy density of 160 mJ/cm^2 [6]. The gratings had a length of 5 mm and a transmission strength 10 dB approximately. To allow for multiplexed interrogation of the grating sensors, we used different phase masks with periods 1073.2, 1067.73 and 1064.7 nm resulting in FBGs with reflection bands in the 1540-1555 nm range. The spatial location of the FBGs along the fiber length differed, depending upon the desired sensor positioning along the composite shaft. Following inscription, the FBGs were annealed at a temperature of 250 °C to demarcate temperature induced refractive index changes, during thermal curing processing.

We manufactured cylindrical carbon fiber shafts [5] with a filament winding process using a pre-programmed robotic arm that applies a number of resin-immersed carbon fibers onto a metal spinning mandrel at a specific inclination angle and a dedicated layup. During the winding process, which is almost fully automatic and required very little human intervention, the robot arm was paused whenever a FBG or FBG array had to be manually positioned. Care was taken to maintain the FBG's orientation during continuation of the winding process. The optical fibers had reinforced egress points (through the outer surface of the shaft) with a PTFE tube (ID 0.3mm, OD 0.6mm).The mandrel was then cured inside an oven whilst being continuously rotated. Following curing the mandrel was extracted by mechanical force, leaving a filament wound hollow shaft. We obtained a 2m long shaft fabricated with a 55^o helical-winding pattern, a wall thickness of 3.06 mm and external diameter of 49.6 mm which was then diamond-cut to produce two separate shafts A and B with embedded sensors. In addition to the embedded gratings, we surface-mounted gratings to the two shafts using adhesive X120 (HBM) to allow for comparison of the response of embedded and external gratings.

Fig. 1 shows a schematic of the orientation of the gratings along the two shafts. Shaft A, that had a length of 89cm, was equipped with two embedded gratings aligned with the carbon fibers at 55^o (FBG A1 & FBG A2) and one surface-mounted grating (FBG A3) with the same orientation (Fig. 1(a)). These gratings were positioned 54 and 73 cm from the shaft edge respectively. Shaft B, with 114 cm length, held one grating that was placed circumferentially at 68 cm (FBG B1) and a grating array with 3 gratings oriented longitudinally. During manufacturing this fiber array fractured however, leaving only one longitudinal grating (FBG B2) positioned 84 cm from the shaft edge. We also mounted an external circumferential grating (FBG B3) at the same axial location as the embedded one (Fig. 1(b)). For each shaft the FBGs were multiplexed to allow interrogation of all sensors simultaneously.

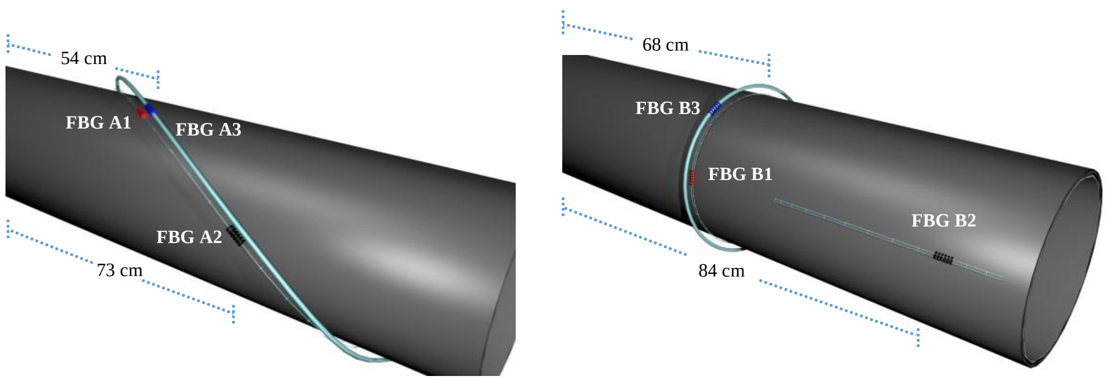

Fig. 1. Schematic (not in scale) of the optical fiber Bragg sensor orientation along the composite shafts (a) Shaft A, (b) Shaft B. Solid fiber lines denote FBGs externally attached to the shaft and wireframe fiber lines denote FBGs embedded in the shaft.

To test the behavior of the FBG sensors under increasing torque, we fixed the shafts as shown in Fig. 2 with one end securely clamped, while a 5% precision torque wrench was attached at the other end. The torque wrench was set to a pre-defined value that was then manually applied to the shaft. The max torque value was increased with consecutive steps up to 900 Nm, while the FBG reflection spectra were acquired in real time at a 10Hz acquisition rate using an Ibsen IMON 256USB FBG interrogator and an amplified spontaneous emission (ASE) broadband light source.

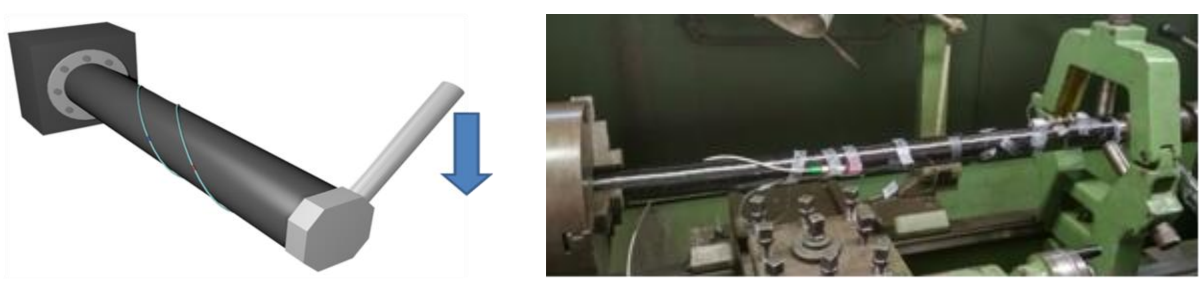

Fig. 2. (a) Torque tests experimental set up for buckling sensor development, (b) Torque experiment

3. Results and Discussion

Table I lists a comparison of the wavelength shifts of the embedded FBGs with respect to their orientation in the composite matrix before and after the curing cycle. The highest shift of 1.7 nm is recorded for the grating with longitudinal orientation.

Table I: Wavelength shifts of embedded FBGs for different orientations with respect to the composite shaft.

Fiber orientation	**0^o**	**55^o**	**55^o**	**90^o**
Grating label	FBG B1	FBG A1	FBG A2	FBG B2
Wavelength after installation (nm)	1545.256	1545.256	1551.728	1552.420
Wavelength after curing (nm)	1543.550	1544.380	1551.030	1551.900
Wavelength shift (nm)	-1.706	-0.876	-0.698	-0.520

The mechanical force extraction of the shaft from the mandrel did not induce a measurable shift of the peak wavelengths of the FBGs. Following attachment of the external FBGs, the sensor spectra for both shafts were recorded as shown in Fig. 3 (a) and (b) for Shaft A and B, respectively.

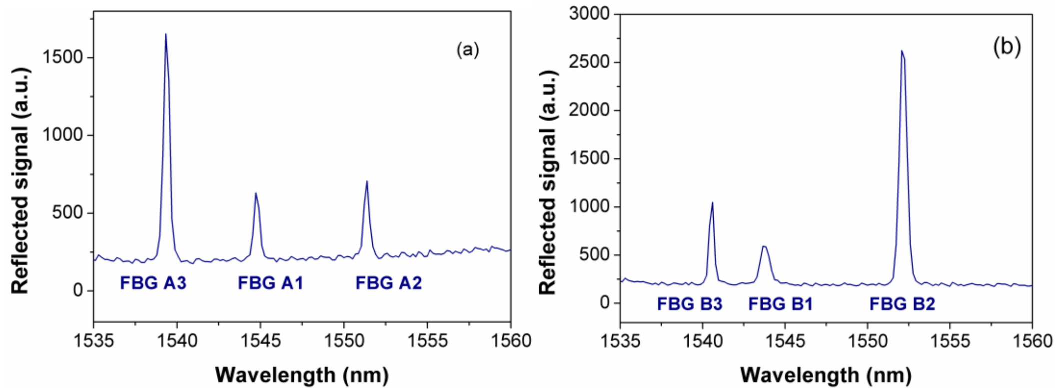

Fig. 3. Reflection spectra of the embedded / attached FBG sensors (a) shaft A, all FBG at 55^o, FBG A1& A2 embedded, FBG A3 external (b) shaft B, FBG B1 circumferential /embedded, FBG B2 longitudinal /embedded, FBG B3 circumferential/external.

The spectral shifts recorded for increasing levels of torque are depicted in Fig. 4 (a) and (c) for the sensors of Shaft A and B respectively. The corresponding maximum Bragg wavelength shifts measured versus torque are plotted in Fig 4 (b) and (d). For shaft B the maximum torque that could be applied was 550 Nm since for higher levels the metallic fixtures glued at the end of the shaft to facilitate the measurement disconnected. No shaft deformation was visually detected for the torque levels applied. As shown, the recorded grating wavelength shifts increase with torque. All FBGs exhibit red wavelength shifts except for the surface-mounted circumferential FBG on shaft B (FBG B3).

Comparing the two shafts for the same level of torque e.g. 500 Nm, the FBGs oriented parallel to the carbon fibers at 55^o exhibit around 3 times larger shift versus those placed longitudinally or circumferentially on shaft B. For shaft A the difference in shift recorded by the embedded / externally attached sensors (FBG 1& 3) is less than 0.1nm on average. In shaft B there is a substantial difference between the circumferential embedded and externally attached FBGs B1 & 3. FBG B3 at the surface of the shaft exhibits a blue shift indicative of compression of the shaft at the specific location. Although the two FBGs are placed at the same location along the shaft their exact circumferential location is uncertain and therefore direct comparison is not possible. Finite elements structural simulations are currently carried out to further investigate the behavior of the composite shafts under torque and will be correlated with the experimental data.

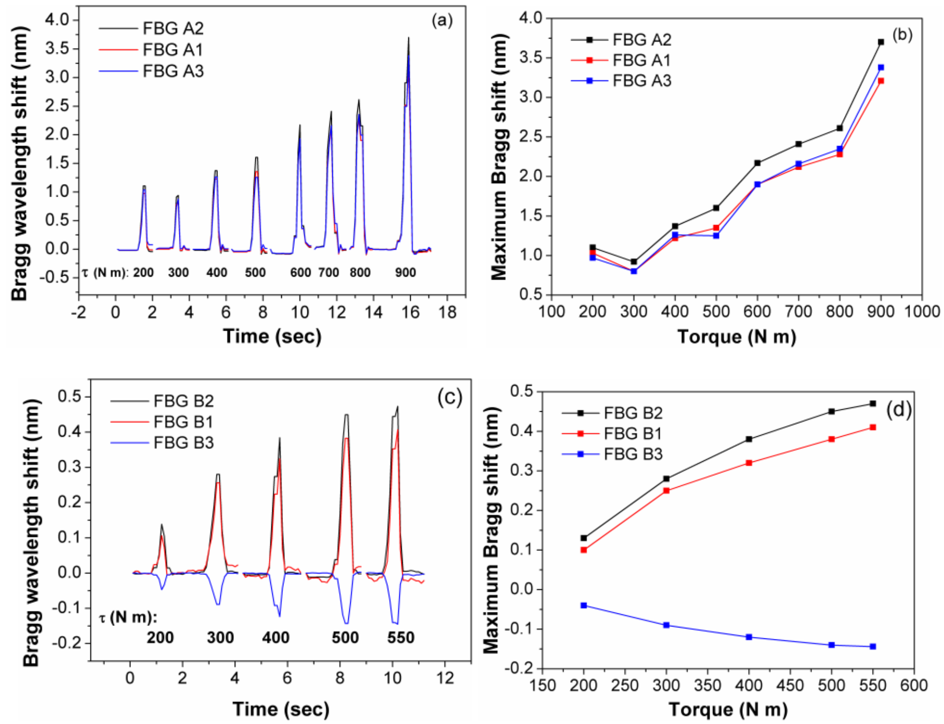

Fig. 4. (a) Bragg wavelength spectral shifts under increasing level of torque τ for the gratings of Shaft A and (b) maximum Bragg wavelength shift versus torque for Shaft A, (c) and (d) as above for shaft B

4. Conclusions

We report results on the use of fiber Bragg grating sensors embedded in carbon fiber composite driveshafts fabricated by filament winding. We studied the response of the fiber Bragg gratings, having different orientations with respect to the shaft axis, under torque loading. Such measurements could provide insight into the buckling experienced by the shafts. To the best of our knowledge this is the first demonstration of strain sensing with Bragg gratings embedded in a filament wound composite shaft under a torsional load.

Acknowledgment: The work presented has been performed within the framework of "ACTPHAST - Access Center for Photonics Innovation Solutions and Technology Support". This project has received funding from the European Union's Seventh Framework Programme for research, technological development and demonstration under Grant Agreement n°619205. GV and NK acknowledge the financial support of the Stavros Niarchos Foundation within the framework of the project ARCHERS ("Advancing Young Researchers' Human Capital in Cutting Edge Technologies in the Preservation of Cultural Heritage and the Tackling of Societal Challenges"). The authors from VUB would like to acknowledge financial support from the Methusalem and Hercules Foundations as well as the Belgian Science Policy Interuniversity Attraction Pole P7/35.

5. References

[1] C. Sonnenfeld, S. Sulejmani, T. Geernaert, S. Eve, N. Lammens, G. Luyckx, E. Voet, J. Degrieck, W. Urbanczyk, P. Mergo, M. Becker, H. Bartelt, F. Berghmans, and H. Thienpont, "Microstructured Optical Fiber Sensors Embedded in a Laminate Composite for Smart Material Applications," Sensors 11, 2566–2579 (2011).

[2] Ch. Riziotis1, L. Eineder, L. Bancallari, and G, Tussiwand "Fiber Optic Architectures for Strain Monitoring of Solid Rocket Motors' Propellant" Sensors Let. 11, 1–5 (2013)

[3] D. Kinet, P. Mégret, K. Goossen, L. Qiu, D. Heider, and C. Caucheteur, "Fiber Bragg Grating Sensors toward Structural Health Monitoring in Composite Materials: Challenges and Solutions," Sensors 14, 7394–7419 (2014).

[4] M. Majumder, T.K. Gangopadhyay, A.K. Chakraborty, K. Dasgupta, D.K. Bhattacharya "Fiber Bragg gratings in structural health monitoring-present status and applications" Sens. Actuators A Phys., 147, pp. 150-164 (2008).

[5] All composite shafts were fabricated at the premises of B&T Composites S.A. at Florina, Greece

[6] M. Konstantaki, P. Childs, M. Sozzi, and S. Pissadakis, S. "Relief Bragg reflectors inscribed on the capillary walls of solid-core photonic crystal fibers" Laser & Photonics Reviews, 7, 439-443 (2013)